

NUMERICAL SCHEME FOR TRANSIENT SEEPAGE ANALYSIS UNDER UNSATURATED CONDITIONS

Pham Nguyen Linh Khanh^{a,b,*}, Nguyen Hoai Nghia^{a,b}

^aInternational University, VNU-HCMC, Quarter 6, Thu Duc city, Ho Chi Minh city, Vietnam

^bVietnam National University Ho Chi Minh City (VNU-HCM),
Linh Trung Ward, Thu Duc city, Ho Chi Minh city, Vietnam

Article history:

Received 01/7/2021, Revised 12/01/2022, Accepted 13/01/2022

Abstract

Unsaturated soil behaviors characterize the failure mechanisms of geotechnical infrastructures with transient seepage conditions. Therefore, an accurate estimate of the unsaturated groundwater flow is vital in improving hazard management and assessment. This study attempts to develop a numerical scheme for 2-D transient analysis under unsaturated conditions. First, the unsaturated groundwater flow was described using the mass conservation law. Then, the Finite Difference Method and Backward Euler approximation were applied for space and time discretization, respectively. Furthermore, the simple Picard iteration was applied to linearize the governing equation. The reliability of the presented method was verified with the analytical solution. The evaluation results demonstrated the sufficiency of the proposed method, quantitatively expressed by the maximum error of 0.04% for opened boundary conditions and 0.15% for closed boundary conditions. The significant advantage of the proposed method is the flexibility with various soil-water characteristic curve models and associated hydraulic conductivity functions, which helps to improve the applicability in practice.

Keywords: unsaturated groundwater flow; Richards equation; rainfall infiltration, 2-D Richards solution.

[https://doi.org/10.31814/stce.huce\(nuce\)2022-16\(1\)-08](https://doi.org/10.31814/stce.huce(nuce)2022-16(1)-08) © 2022 Hanoi University of Civil Engineering (HUCE)

1. Introduction

Groundwater can flow exclusively through the pore space filled with water. Thus, the hydraulic conductivity of unsaturated soils clearly depends on volumetric water content θ and matric suction (ψ). Modeling unsaturated groundwater flow is based on the mass conservation law for the water phase, a given soil water characteristic curve (SWCC) model, and the associated hydraulic conductivity function (HCF). Due to the dependence of θ and hydraulic conductivity ψ , the mass conservation equation becomes highly nonlinear, well known as the Richards equation. Many studies have attempted to solve the Richards equation analytically and numerically.

Most analytical solutions employ the exponential SWCC model and Gardner's HCF (1958) because of their linearization capability [1]. Based on the one-dimensional analytical solution for the vertical rainfall infiltration proposed by Srivastava and Yeh [2], Zhan and Ng [3] conducted a parametric study to assess the influence of hydraulic parameters on the infiltration mechanism into unsaturated soils. The analytical solutions were also commonly used in stability analysis for a partially saturated slope induced by rainfall infiltration [4, 5].

*Corresponding author. E-mail address: pnlkhanh@hcmiu.edu.vn (Khanh, P. N. L.)

On the contrary, numerical analyses provide significant flexibility in the choice of both the SWCC model and HCF. The nonlinear governing equation of unsaturated groundwater flow can be linearized under iterative schemes, e.g., Picard, modified Picard, and Newton-Raphson. Additionally, computational techniques, e.g., finite difference method [6], finite element method [7], finite volume method [8], or coupled finite-discrete element method [9], are adopted to solve these problems approximately. The general mixed-form of the Richards equation was suggested for a perfectly conserved solution [6]. Moreover, a great effort was also made to enhance the numerical scheme [10].

This paper developed a numerical scheme for transient analysis under unsaturated conditions. First, the mass conservation law was applied to describe the unsaturated groundwater flow. Then, the finite difference method and backward Euler approximation were utilized for space and time discretization. Also, the nonlinearity of the governing equation resulting from the inclusion of the SWCC model and its associated HCF was linearized using the simple Picard iteration. Finally, an analytical solution with different hydraulic boundary conditions verified the presented model’s performance.

2. Materials

The recycled aggregate is widely used and regarded as an economical backfill material for geotechnical constructions, in which groundwater flow has an utmost important role. For the laboratory experiment, four different recycled aggregate samples were collected from different areas. The dry unit weight of the recycled aggregate is 1.566-1.785 (g/m³). The samples were initially oven-dried at 95 °C for 48 (hr) and then mixed with distilled water. Before conducting the pressure plate extractor (PPE) tests, the samples were kept in a humidity-controlled desiccator for 24 (hr) to ensure uniform water distribution. The size of the samples was 10 (mm) in height and 50.2 (mm) in diameter.

Table 1. Summary of SWCC models, relative hydraulic conductivity, and specific moisture capacity

SWCC Model	Effective volumetric water content	Relative hydraulic conductivity function	Specific moisture capacity
Brooks and Corey [11]	$S_e = \begin{cases} (\psi/\psi_b)^{-\lambda} & \psi > \psi_b \\ 1 & \psi \leq \psi_b \end{cases}$	$K_r = \begin{cases} (\psi/\psi_b)^{-(2+\tau\lambda+2\lambda)} & \psi > \psi_b \\ 1 & \psi \leq \psi_b \end{cases}$	$S = -\lambda(\theta_S - \theta_R) \frac{\psi^{-\lambda-1}}{\psi_b^{-\lambda}}$
Van Genuchten [12]	$S_e = \frac{1}{[1 + (\alpha\psi)^n]^m}$	$K_r = S_e^{\tau} [1 - (1 - S_e^{1/m})^m]^2$	$S = \frac{-mn(\alpha\psi)^n}{\psi[1 + (\alpha\psi)^n]^{m+1}} (\theta_S - \theta_R)$
Kosugi [13]	$S_e = \frac{1}{2} \operatorname{erfc} \left(\frac{\ln(\psi/\psi_m)}{\sqrt{2}\sigma} \right)$	$K_r = S_e^{1/2} \left[\frac{1}{2} \operatorname{erfc} \left(\frac{\ln(\psi/\psi_m) + \sigma^2}{\sqrt{2}\sigma} \right) \right]^2$	$S = \frac{\theta_R - \theta_S}{\psi \sqrt{2\pi}\sigma} e^{-\left(\frac{\ln(\psi/\psi_m)}{\sqrt{2}\sigma}\right)^2}$
Fredlund and Xing [14]	$\theta = C(\psi) \frac{\theta_S}{\{\ln[e + (\psi/a)^n]\}^m}$ $C(\psi) = \frac{-\ln(1 + \psi/\psi_r)}{\ln(1 + 10^6/\psi_r)} + 1$	$K_r = \frac{\int_{\ln(\psi)}^b \frac{\theta(e^y) - \theta(\psi)}{e^y} \theta'(e^y) dy}{\int_{\ln(\psi_{aev})}^b \frac{\theta(e^y) - \theta_S}{e^y} \theta'(e^y) dy}$	$S = C'(\psi) \frac{\theta_S}{\{\ln[e + (\psi/a)^n]\}^m} - C(\psi) \frac{\theta_S}{\{\ln[e + (\psi/a)^n]\}^{m+1}} \times \frac{mn(\psi/a)^{n-1}}{a[e + (\psi/a)^n]}$
Exponential model	$S_e = e^{\alpha\psi}$	$K_r = e^{\alpha\psi}$	$S = \alpha(\theta_S - \theta_R) e^{\alpha\psi}$

* $\theta = \theta_R + (\theta_S - \theta_R) S_e$; D.G. Fredlund and Xing (1994): $C'(\psi) = \frac{-1}{(\psi_r + \psi) \ln(1 + 10^6/\psi_r)}$.

A series of PPE tests were carried out complying with the standard procedure of ASTM 3152 to determine the correlation between θ and matric suction. Matric suction increment was controlled by air pressure along with the axis-translation technique. Principal components of the PPE apparatus include a pressure chamber, pressure control equipment, and ceramic disks. During the experiment, the air pressure was gradually applied to drain the pore water out through the ceramic disks placed at the bottom of the specimens. This process continued until the equilibrium state was held by the matric suction, and the volumetric water content of the samples was then measured. This procedure was repeated to determine the correlation between θ and matric suction. Based on the experimental results, model parameters of the SWCC models, as summarized in Table 1, were determined by the nonlinear curve-fitting program of Soilvision. Note that θ_R and θ_S are the volumetric water content of sample at the residual state and saturated state, respectively; $\lambda, h_b, \alpha, n, m, h_m$, and σ are model parameters determined by curve-fitting technique; K_s is the saturated hydraulic conductivity (L/T). Table 2 shows the determined model parameters of each SWCC model for the four samples.

Table 2. Model parameters of SWCC models obtained by a curve-fitting technique

SWCC models	Parameters	Sample			
		1	2	3	4
Van Genuchten [12]	θ_S	0.0877	0.0715	0.0814	0.0788
	θ_R	0.0037	0.0027	0.0079	0.0053
	α	0.0061	0.0033	0.0092	0.0067
	n	1.6284	1.4444	1.3875	1.5083
Kosugi [13]	θ_S	0.0879	0.0717	0.0817	0.0789
	θ_R	0.0059	0.0066	0.0125	0.0082
	h_m	465.01	1308.9	601.59	549.54
	σ	1.5301	1.8968	2.0649	1.7478
Brooks and Corey [11]	θ_S	0.0869	0.0709	0.0806	0.0782
	θ_R	0.0016	5.51×10^{-5}	0.0042	0.0021
	h_b	94.842	151.84	59.416	76.004
	λ	0.4671	0.3143	0.2884	0.3576
Fredlund and Xing [14]	θ_S	0.08772	0.0715	0.0812	0.0786
	a	220.59	463.03	133.55	166.41
	m	1.2503	1.1090	0.7168	0.8267
	n	1.3895	1.1845	1.4790	1.666
Exponential model	θ_S	0.0875	0.0704	0.0793	0.0786
	θ_R	0.0038	0.0081	0.0142	0.0112
	α	0.0013	0.0005	0.001	0.0015

Figs. 1 and 2 show the determined SWCC models and the relationship between specific moisture capacity (S) and matric suction, respectively. The specific moisture capacity means the rate of change of θ on the pore water pressure. The correlation between the SWCC models and the experimental data was evaluated by examining the Nash-Sutcliffe efficiency coefficient (\bar{R}^2). Based on the assessment result, as shown in Table 3, the exponential SWCC model shows a relatively inferior correlation with the experimental results among the SWCC models considered. Especially, this tendency was more clearly demonstrated in the case of the relationship between S and matric suction, as shown in Fig. 2. Going into details, the exponential SWCC model yielded the lowest average and maximum \bar{R}^2 for all of the four samples ($\bar{R}^2 = 0.9822, R_{\max}^2 = 0.9861$); on the other hand, the other SWCC models showed these values above 0.9992. Especially, the Fredlund and Xing [14] SWCC model best fitted the experimental data ($\bar{R}^2 = 0.9993; R_{\min}^2 = 0.9986$), which is the most suitable for the recycled aggregate samples. No doubt that the more the model parameters involved in the SWCC model, the better it fits the experimental results: 3 in the Fredlund and Xing [14] SWCC model, and 1 in the exponential SWCC model. However, many model parameters lead to a more complicated and highly nonlinear form of the Richards equation. Besides, close observation on Figs. 1 and 2 indicates that the transition from saturated to unsaturated conditions is not smooth in the Brooks and Corey [11] SWCC model.

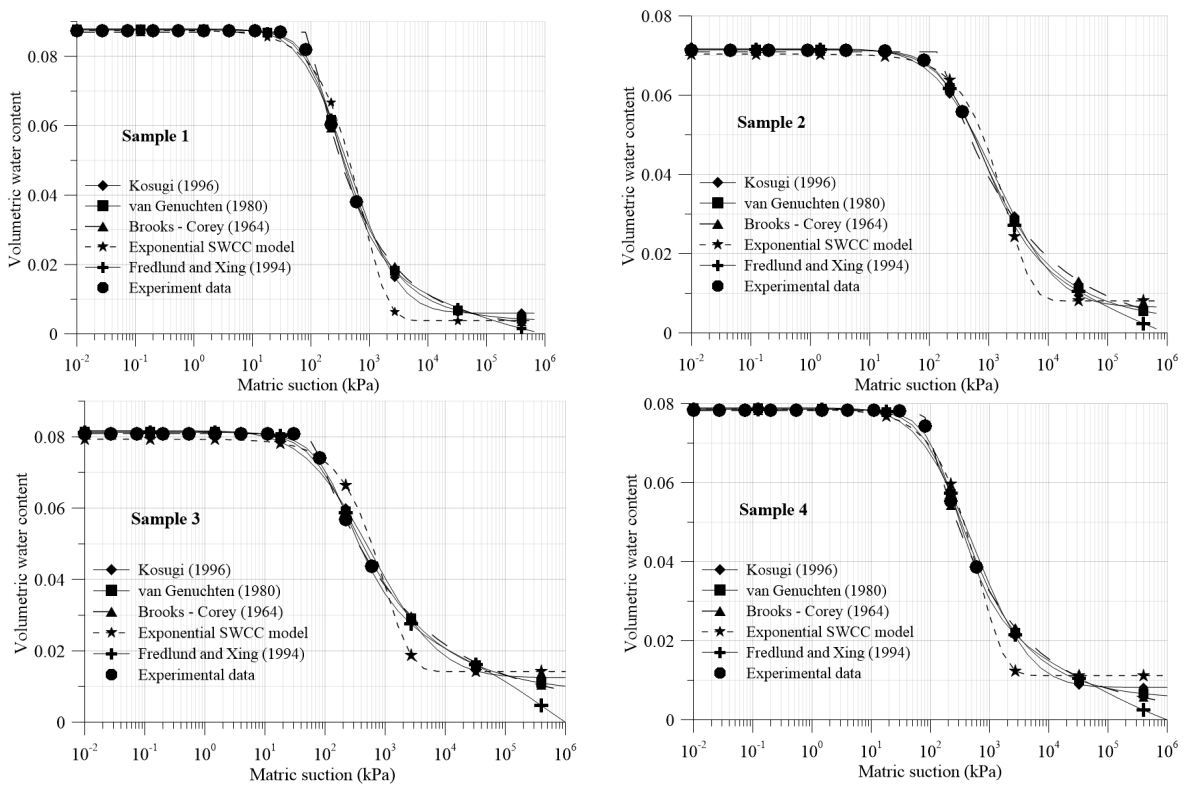


Figure 1. SWCC models correlated to experimental results

Fig. 3 shows a relationship between relative unsaturated hydraulic conductivity and matric suction. Even though the SWCC models closely matched each other, as illustrated in Fig. 1, the relative hydraulic conductivity significantly differed at the same matric suction.

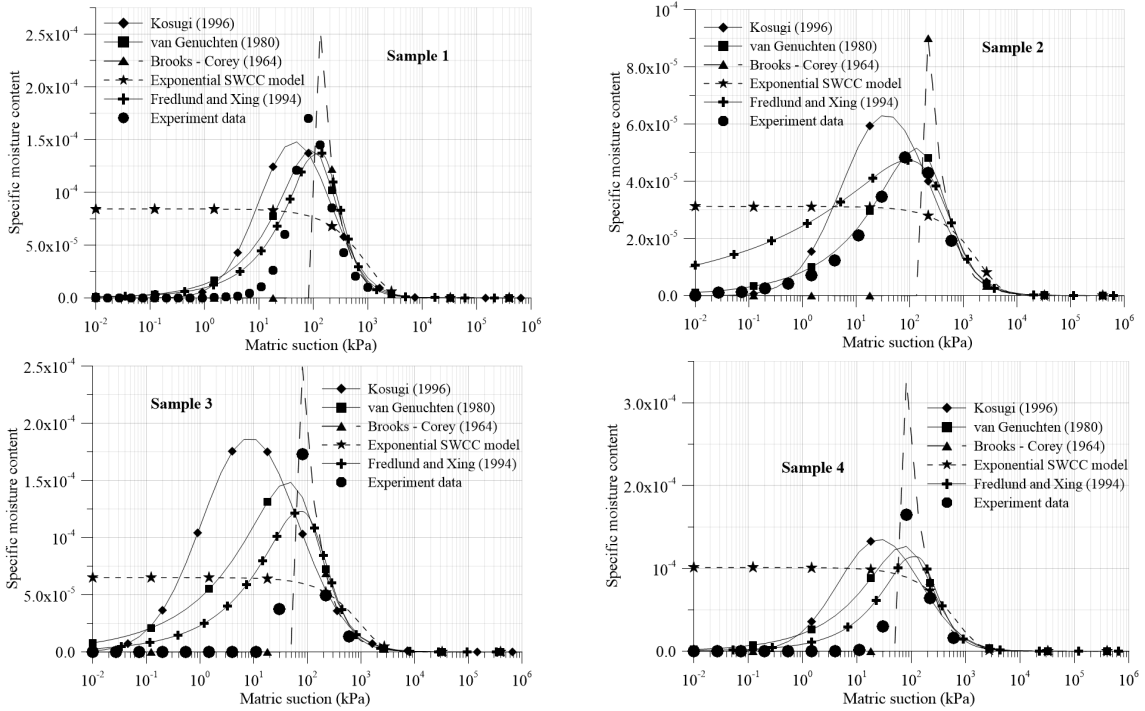


Figure 2. Relationship between specific moisture capacity and matric suction

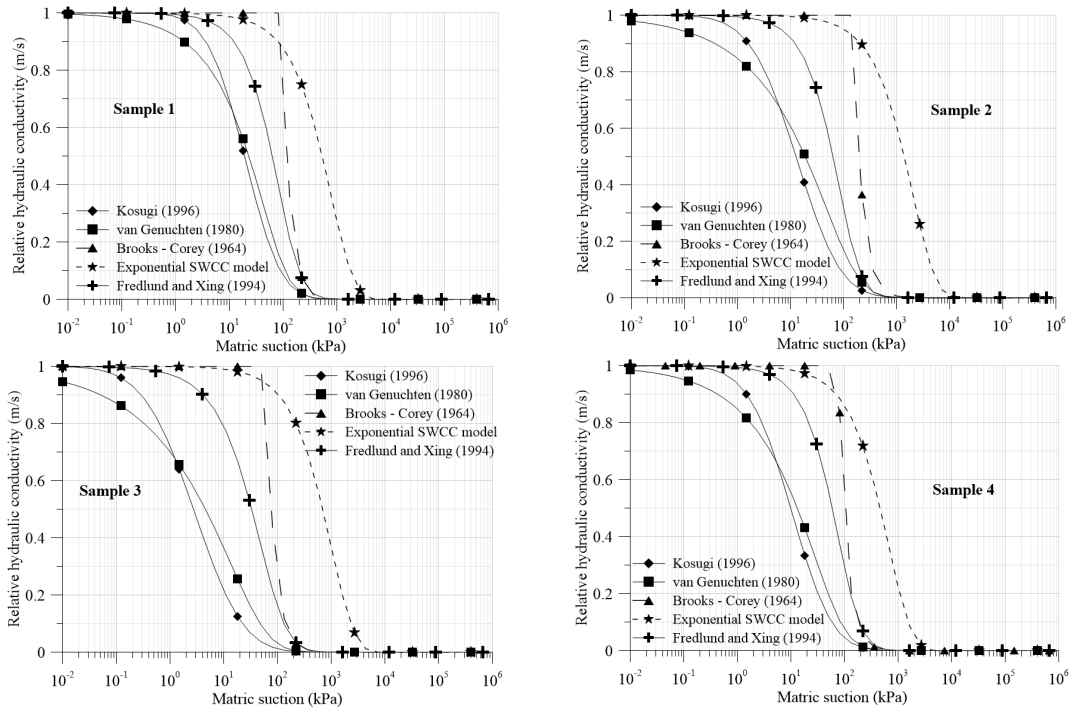


Figure 3. Relationship between relative hydraulic conductivity and matric suction

Table 3. Correlation between SWCC models and experimental data

*Nash-Sutcliffe efficiency coefficient (R^2)	Sample 1	Sample 2	Sample 3	Sample 4
Van Genuchten [12]	0.9994	0.9999	0.9983	0.9987
Kosugi [13]	0.9970	0.9984	0.9939	0.9953
Brooks and Corey [11]	0.9993	0.9977	0.9999	0.9997
D.G. Fredlund and Xing [14]	0.9995	0.9998	0.9986	0.9992
Exponential	0.9861	0.9849	0.9736	0.9842

$$*R^2 = 1 - \frac{\sum_{i=1}^n (obs_i - sim_i)^2}{\sum_{i=1}^n (obs_i - \overline{obs_i})^2}$$

3. Numerical modeling

3.1. General mixed-form Picard iteration for 2-D unsaturated groundwater flow

Among three popular forms of the Richards equation, i.e., h -based form, θ -based form, and mixed-form, Celia et al. [6] recommended using the mixed-form expressed as Eq. (1), because it ensures the mass conservation and requires no additional computational effort than the standard h -based form.

$$\frac{\partial \theta}{\partial t} dV = \nabla \cdot \mathbf{q} \quad (1)$$

where dV is the volume of element (L^3), $\mathbf{q} = [q_x \ q_y]^T$ is the fluid flow (L^3/T), t is the time (T). To numerically solve Eq. (1) in two dimensions, the standard FDM and backward Euler approximation were utilized for space and time discretization, respectively, as follows:

$$\begin{aligned} \nabla \cdot \mathbf{q} &= \frac{\partial q_x}{\partial x} dx + \frac{\partial q_y}{\partial y} dy \\ &\approx \frac{(q_x)_{i,j+1/2} - (q_x)_{i,j-1/2}}{\Delta x} dx + \frac{(q_y)_{i+1/2,j} - (q_y)_{i-1/2,j}}{\Delta y} dy \\ (i = 1 \dots n_y; j = 1 \dots n_x) \frac{\partial \theta}{\partial t} &\approx \frac{\theta^{n+1} - \theta^n}{\Delta t} \end{aligned} \quad (2)$$

where $\Delta x, \Delta y$ = space interval between nodes in the x and y direction, respectively (L); n_x, n_y = number of space interval in x and y direction, respectively; n = time step; Δt = time increment (T).

Under unsaturated conditions, Darcy law can also describe the fluid flow rate. However, the value of hydraulic conductivity, at this time, depends on the matric suction or ψ .

$$\begin{aligned} q_x &= K_x(\psi) \frac{\partial h}{\partial x} A_{yz} = K_x(\psi) \frac{\partial \psi}{\partial x} A_{yz} \\ q_y &= K_y(\psi) \frac{\partial h}{\partial y} A_{xz} = K_y(\psi) \left(\frac{\partial \psi}{\partial y} + 1 \right) A_{xz} \end{aligned} \quad (3)$$

where h = total hydraulic head (L); A_{xy}, A_{yx} = cross-sectional areas, which are orthogonal to the corresponding fluid flows (L^2).

Inserting Eq. (3) into the first term of Eq. (2), then the right-hand side (RHS) of Eq. (1) becomes:

$$\begin{aligned}
 RHS = & \frac{(K_y)_{i+1/2,j}}{\Delta y^2} \psi_{i+1,j} - \left[\frac{(K_y)_{i+1/2,j} + (K_y)_{i-1/2,j}}{\Delta y^2} + \frac{(K_x)_{i,j+1/2} + (K_x)_{i,j-1/2}}{\Delta x^2} \right] \psi_{i,j} \\
 & + \frac{(K_y)_{i-1/2,j}}{\Delta y^2} \psi_{i-1,j} + \frac{(K_x)_{i,j+1/2}}{\Delta x^2} \psi_{i,j+1} + \frac{(K_x)_{i,j-1/2}}{\Delta x^2} \psi_{i,j-1} + \frac{(K_y)_{i+1/2,j} - (K_y)_{i-1/2,j}}{\Delta y}
 \end{aligned} \tag{4}$$

where K_x, K_y = hydraulic conductivity in x, y direction, respectively (L/T).

Because θ and K depend on ψ , Eq. (1) is nonlinear so that the simple Picard iteration method was applied to linearize this equation. Furthermore, Celia et al. [6] suggested utilizing the truncated Taylor series to fully ensure mass conservation to expand $\theta^{n+1,m+1}$ (m = iterative step) ψ . Finally, the numerical scheme for solving the mixed-form Richards equation in two dimensions is described as follows:

$$\begin{aligned}
 LHS = & -\frac{(K_y)_{i+1/2,j}^{n+1,m}}{\Delta y^2} \delta_{i+1,j}^m + \left[A + \frac{S_{i,j}^{n+1,m}}{\Delta t} \right] \delta_{i,j}^m - \frac{(K_y)_{i-1/2,j}^{n+1,m}}{\Delta y^2} \delta_{i-1,j}^m \quad (\delta_{i,j}^m = \psi_{i,j}^{n+1,m+1} - \psi_{i,j}^{n+1,m}) \\
 RHS = & \frac{(K_y)_{i+1/2,j}^{n+1,m}}{\Delta y^2} \psi_{i+1,j}^{n+1,m} - [A] \psi_{i,j}^{n+1,m} + \frac{(K_y)_{i-1/2,j}^{n+1,m}}{\Delta y^2} \psi_{i-1,j}^{n+1,m} + \frac{(K_x)_{i,j+1/2}^{n+1,m}}{\Delta x^2} \psi_{i,j+1}^{n+1,m} \\
 & + \frac{(K_x)_{i,j-1/2}^{n+1,m}}{\Delta x^2} \psi_{i,j-1}^{n+1,m} + \dots + \frac{(K_y)_{i+1/2,j}^{n+1,m} - (K_y)_{i-1/2,j}^{n+1,m}}{\Delta y} + \frac{\theta_{i,j}^n - \theta_{i,j}^{n+1,m}}{\Delta t} \\
 A = & \frac{(K_y)_{i+1/2,j}^{n+1,m} + (K_y)_{i-1/2,j}^{n+1,m}}{\Delta y^2} + \frac{(K_x)_{i,j+1/2}^{n+1,m} + (K_x)_{i,j-1/2}^{n+1,m}}{\Delta x^2}
 \end{aligned} \tag{5}$$

For a given initial condition, the increment of ψ at each node ($\delta_{i,j}^m$) after every iterative step can be obtained by solving Eq. (5). The value of ψ along with θ, K and S should be updated for the next iteration step. This procedure repeats until a given convergence criterion is satisfied. Among widely-used convergence criteria, Huang et al. [15] proposed a criterion based on the value of θ as Eq. (6) to enhance the numerical performance.

$$\left| \theta_{i,j}^{n+1,m+1} - \theta_{i,j}^{n+1,m} \right| \leq \delta_\theta \tag{6}$$

where δ_θ = given tolerance.

It is of interest that when representing Eq. (5) in a matrix form, the coefficient matrix is tridiagonal. Therefore, to reduce the computational cost, one does not need to store the full square matrix, but only for the non-zero components, as three vectors.

The value of hydraulic conductivity between two adjacent nodes can be estimated by one of the following two methods: (i) based on the geometric mean of ψ at the two nodes in a given direction or (ii) based on the geometric mean of the hydraulic conductivity values at each node in a given direction. In addition, a weight function can enhance interpolation accuracy, which was discussed in detail by Van Dam and Feddes [10]. According to the numerical experiment, this study suggested applying the latter method.

Regarding the boundary conditions for unsaturated groundwater flow problems, the Dirichlet boundary conditions resulted in a similar computation process in saturated conditions. However, when dealing with the Neumann boundary conditions, the conventional techniques for saturated conditions,

such as pseudo nodes and one-sided differences, cannot be directly applied because the unsaturated hydraulic conductivity depends on θ or ψ . For example, in the case of a rainfall infiltration problem when a vertical flow rate on the surface boundary is given, the Neumann boundary conditions can be treated as follows:

$$\begin{aligned} \frac{\partial q_y}{\partial y} &= \frac{(q_y)_{i+1/2,j} - (q_y)_{i-1/2,j}}{\Delta y} = \frac{q_y^{in}}{\Delta y} - \frac{(K_y)_{i-1/2,j}}{\Delta y^2} (\psi_{i,j} - \psi_{i-1,j}) - \frac{(K_y)_{i-1/2,j}}{\Delta y} \\ \frac{\partial q_x}{\partial x} &= \frac{(K_x)_{i,j+1/2}}{\Delta x^2} \psi_{i,j+1} - \frac{(K_x)_{i,j+1/2} + (K_x)_{i,j-1/2}}{\Delta x^2} \psi_{i,j} - \frac{(K_x)_{i,j-1/2}}{\Delta x^2} \psi_{i,j-1} \end{aligned} \quad (7)$$

Inserting Eq. (7) into Eq. (1), the computational procedure for these surface nodes can be ordinarily implemented. Furthermore, when the volumetric water content at these nodes equals to θ_s , the run-off phenomenon is assumed to occur.

3.2. Model validation

The developed numerical scheme was adopted to estimate the hydraulic response of an unsaturated soil column, with the height of L (m) and the width of a (m), to a specific pore water pressure head. The initial condition of the soil column was dry, i.e. $\psi(x, z, 0) = \psi_d < 0$, before the hydraulic pressure head was applied to the top boundary. This problem is called 2-D Green-Ampt. problem [16]. The analytical solution presented by Tracy [1] was employed to verify the numerical model, in which the exponential SWCC model and the Gardner [17] HCF were used. The hydraulic response of the soil column was estimated on two types of boundary conditions as follows:

- Open-flow through the domain sides' boundary conditions:

$$\begin{aligned} \psi(0, z, y) &= \psi(a, z, t) = \psi(x, 0, t) = \psi_d \\ \psi(x, L, t) &= \frac{1}{\alpha} \ln \left(e^{\alpha\psi_d} + (1 - e^{\alpha\psi_d}) \sin \frac{\pi x}{a} \right) \end{aligned} \quad (8)$$

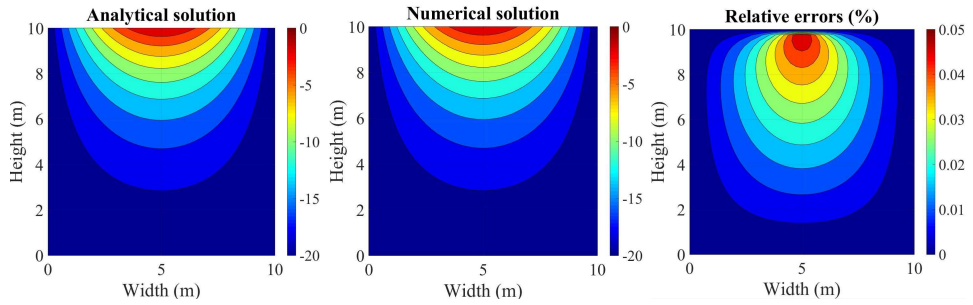
- Close-flow through the domain sides' boundary conditions:

$$\begin{aligned} \psi(x, 0, t) &= \psi_d \\ \psi(x, L, t) &= \frac{1}{\alpha} \ln \left(e^{\alpha\psi_d} + \frac{1 - e^{\alpha\psi_d}}{2} \left(1 - \cos \frac{2\pi x}{a} \right) \right) \end{aligned} \quad (9)$$

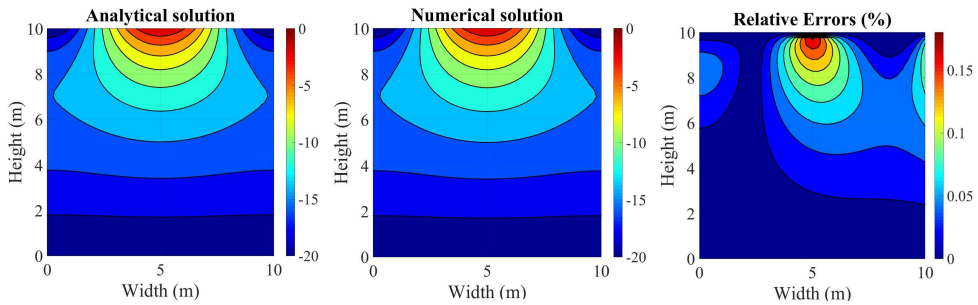
Model parameters for the exponential SWCC model of Sample 1 and Sample 2, from the soil water retention test, were chosen for calculation, which are summarized in Table 4.

Table 4. Modeling parameters used for validating numerical scheme

Parameters	Unit	Sample 1	Sample 2
a	m	10	10
L	m	10	10
h_d	m	-20	-20
α	kPa ⁻¹	0.0013	0.0005
θ_S	-	0.0875	0.0704
θ_R	-	0.0038	0.0081
K_S	m/day	0.3	0.3

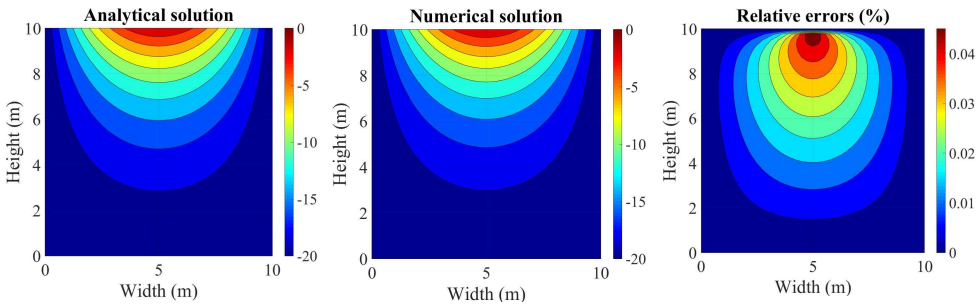


(a) Open-flow sides' boundary conditions

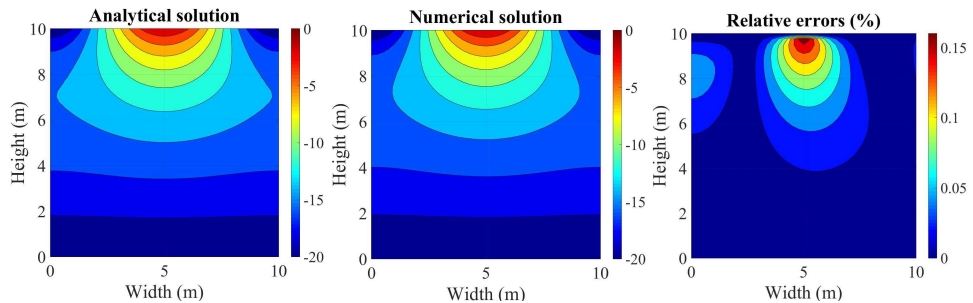


(b) Close-flow sides' boundary conditions

Figure 4. Analytical solutions, numerical solutions and relative errors for Sample 1



(a) Open-flow sides' boundary conditions



(b) Close-flow sides' boundary conditions

Figure 5. Analytical solutions, numerical solutions and relative errors for Sample 2

Figs. 4 and 5 present the analytical and numerical solutions along with the relative errors between the two solutions, in the cases of Sample 1 and Sample 2, respectively. The verification showed

an excellent agreement between the analytical and numerical solutions. In the case of Sample 1, the maximum relative error for the open-flow and the close-flow sides' boundary conditions were 0.05 (%) and 0.15 (%), respectively. In the case of Sample 2, those of the open-flow and the close-flow sides' boundary conditions were 0.04 (%) and 0.15 (%), respectively. Therefore, the developed numerical model was fairly reliable for solving the two-dimensional unsaturated groundwater flow problems.

4. Conclusions

The results of the PPE tests indicated the inferior performance of the exponential SWCC model, among the SWCC models examined, to mathematically represent the relationship between θ and ψ of the recycled aggregate as the economical backfill material. On the other hand, the Fredlund and Xing [14] SWCC model was the most suitable model. Also, even though the SWCC models examined matched closely to each other, the gaps between the associated HCFs and the specific moisture capacity functions still existed.

Using the 2-D analytical solution suggested by Tracy [1], the developed numerical scheme was demonstrated to be reliable in modeling the unsaturated groundwater flow. The main advantages of the proposed numerical scheme include (i) ability to apply for different types of the SWCC model, the heterogeneity of soil properties, and various boundary conditions; (ii) possibility to detect and switch the rainfall infiltration to run-off mode when the ponding phenomenon occurs on the surface.

Acknowledgment

This research is funded by International University, VNU-HCM under grant number T2020-02-CE.

References

- [1] Tracy, F. T. (2006). [Clean two- and three-dimensional analytical solutions of Richards' equation for testing numerical solvers](#). *Water Resources Research*, 42(8).
- [2] Srivastava, R., Yeh, T.-C. J. (1991). [Analytical solutions for one-dimensional, transient infiltration toward the water table in homogeneous and layered soils](#). *Water Resources Research*, 27(5):753–762.
- [3] Zhan, T. L. T., Ng, C. W. W. (2004). [Analytical Analysis of Rainfall Infiltration Mechanism in Unsaturated Soils](#). *International Journal of Geomechanics*, 4(4):273–284.
- [4] Griffiths, D. V., Lu, N. (2005). [Unsaturated slope stability analysis with steady infiltration or evaporation using elasto-plastic finite elements](#). *International Journal for Numerical and Analytical Methods in Geomechanics*, 29(3):249–267.
- [5] Lu, N., Godt, J. (2008). [Infinite slope stability under steady unsaturated seepage conditions](#). *Water Resources Research*, 44(11).
- [6] Celia, M. A., Bouloutas, E. T., Zarba, R. L. (1990). [A general mass-conservative numerical solution for the unsaturated flow equation](#). *Water Resources Research*, 26(7):1483–1496.
- [7] Solin, P., Kuraz, M. (2011). [Solving the nonstationary Richards equation with adaptive hp-FEM](#). *Advances in Water Resources*, 34(9):1062–1081.
- [8] Herrada, M. A., Gutiérrez-Martín, A., Montanero, J. M. (2014). [Modeling infiltration rates in a saturated/unsaturated soil under the free draining condition](#). *Journal of Hydrology*, 515:10–15.
- [9] Kien, N. T., Trung, V. T., Hoang, N. N. (2021). [Coupled finite-discrete element modeling and potential applications in civil engineering](#). *Journal of Science and Technology in Civil Engineering (STCE) - HUCE*, 15(4):111–122.

- [10] van Dam, J. C., Feddes, R. A. (2000). [Numerical simulation of infiltration, evaporation and shallow groundwater levels with the Richards equation](#). *Journal of Hydrology*, 233(1-4):72–85.
- [11] Brooks, R. H., Corey, A. T. (1964). *Hydraulic properties of porous media*. Colorado State University.
- [12] van Genuchten, M. T. (1980). [A Closed-form Equation for Predicting the Hydraulic Conductivity of Unsaturated Soils](#). *Soil Science Society of America Journal*, 44(5):892–898.
- [13] Kosugi, K. (1996). [Lognormal Distribution Model for Unsaturated Soil Hydraulic Properties](#). *Water Resources Research*, 32(9):2697–2703.
- [14] Fredlund, D. G., Xing, A. (1994). [Erratum: Equations for the soil-water characteristic curve](#). *Canadian Geotechnical Journal*, 31(6):1026–1026.
- [15] Huang, K., Mohanty, B. P., van Genuchten, M. T. (1996). [A new convergence criterion for the modified Picard iteration method to solve the variably saturated flow equation](#). *Journal of Hydrology*, 178(1-4): 69–91.
- [16] Tracy, F. T. (2011). [Analytical and numerical solutions of Richards' equation with discussions on relative hydraulic conductivity](#). In *Hydraulic Conductivity-Issues, Determination and Applications*, IntechOpen.
- [17] Gardner, W. R. (1958). Mathematics of isothermal water conduction in unsaturated soils. *Highway research board special report*, 40:78–87.